University of Wisconsin - Madison

MADPH-95-883
April 1995

On the validity of the reduced Salpeter equation

M. G. Olsson and Siniša Veseli

Department of Physics, University of Wisconsin, Madison, WI 53706

Ken Williams

Continuous Electron Beam Accelerator Facility
Newport News, VA 29606, USA
and
Physics Department, Hampton University, Hampton, VA 29668

Abstract

We adapt a general method to solve both the full and reduced Salpeter equations and systematically explore the conditions under which these two equations give equivalent results in meson dynamics. The effects of constituent mass, angular momentum state, type of interaction, and the nature of confinement are all considered in an effort to clearly delineate the range of validity of the reduced Salpeter approximations. We find that for $J \neq 0$ the solutions are strikingly similar for all constituent masses. For zero angular momentum states the full and reduced Salpeter equations give different results for small quark mass especially with a large additive constant coordinate space potential. We also show that $\frac{1}{m}$ corrections to heavy-light energy levels can be accurately computed with the reduced equation.

1 Introduction

The instantaneous Bethe-Salpeter equation, or Salpeter equation [1], is by far the most commonly employed relativistic wave equation in meson models with fermionic constituents. Until recently, almost all explicit calculations have used a simplified version known as the reduced Salpeter equation. The later becomes identical to the full Salpeter equation if at least one of the constituent masses is infinite.

The reduced Salpeter equation is of the standard eigenvalue (hermitian) type whereas the full equation is not. Its solutions are thus algebraically and numerically simpler than that of the full equation. For example, the reduced equation doesn't have negative energy solutions, nor does it have solutions with zero norm, both of which exist for the full Salpeter equation [2, 3]. More importantly, the reduced equation has variationally stable solutions for a wider range of kernel types than does the full equation [4, 5]. For example, there are no variationally stable solutions to the full Salpeter equation corresponding to pure scalar confinement. The reduced Salpeter equation, on the other hand, has well defined variationally stable solutions with scalar confinement. Also, the reduced equation is equivalent to the "no-pair" equation [6] proposed to cure the "continuum dissociation" problem in relativistic atomic physics. There are therefore historical, practical, and physical reasons for using the reduced equation. We outline here the conditions under which this can be done without sacrificing accuracy.

In the real world the constituent mass is never infinite, so one faces a quantitative question as to the practical region of validity of the reduced Salpeter equation. Our results here establish that for many purposes the reduced Salpeter equation is quite adequate and one can take advantage. An analysis involving heavy-light mesons with c or b quarks, or $b\bar{b}$, $c\bar{c}$, or $s\bar{s}$ onia states, does not incur serious error by using the reduced Salpeter equation. It is only for $J = 0$ states and with small quark masses where there can be significant differences between the full and reduced Salpeter solutions. Dynamical models involving light pseudo-scalar states such as the π, η,

or K mesons can lead to serious errors if the full Salpeter equation is not used.

Our analysis draws heavily upon previous work [5] in which we have adopted Lagaë's method [2] to investigate the nature of full Salpeter solutions. Our principal conclusion was that the only linearly confining potential which yields linear Regge trajectories and has variationally stable solutions is a time component Lorentz vector. This confirms previous work done for the equal mass case [4, 7].

In the present work we use the fact that stable solutions exist for the time component vector confinement in order to estimate the range of applicability of the reduced Salpeter equation. The desirable properties of the time component vector potential in the Salpeter equation does not mean that it should be used as a confinement potential, since it yields wrong sign of the spin-orbit interaction, disagreeing both with QCD and experiment. We also compare solutions to the full equation and its reduced version for an equal mixture of scalar and time component vector confinement. This type of mixed confining kernel has been recently used in [3] for the investigation of weak decays of heavy mesons. The vector confinement stabilizes the scalar confining part up to the case of equal mixtures. Phenomenologically, the scalar confining part is necessary to reduce the P-wave spin-orbit splitting. For this mixed confinement case we also explicitly demonstrate that the reduced Salpeter equation is adequate for the investigation of the heavy-light systems, such as D and B mesons, as well as for heavy onia. We also examine the extent to which $\frac{1}{m}$ corrections to heavy-light systems depend on which wave equation is used. We find that the difference is negligible even for D mesons.

In Section 2 we adapt Lagaë's formalism [2] to the reduced Salpeter equation. Our numerical results are contained in Section 3 where we compare the full and reduced Salpeter solutions for both onia and heavy-light mesons. Our conclusions are summarized in Section 4. In the Appendix A we provide the complete reduced Salpeter radial equations for the three Lorentz type kernels, $\gamma^0 \otimes \gamma^0$ [time component vector], $\mathbf{1} \otimes \mathbf{1}$ [scalar], and $\gamma^\mu \otimes \gamma_\mu$ [full vector].

2 Reduced Salpeter equation

Recently Lagaë has proposed an elegant formalism [2] for the reduction of the full Salpeter equation to a system of equations involving only radial wave functions. One of the nice things about his method is that the transition from full to reduced Salpeter equations can be accomplished easily. In this section we briefly sketch the main points of this formalism as adapted to the reduced Salpeter equation.

We start from the Salpeter equation for a fermion-antifermion system in the CM frame of the bound state,

$$\begin{aligned}\Phi(\mathbf{k}) &= \int \frac{d^3\mathbf{k}'}{(2\pi)^3}\left[\frac{\Lambda_+^1(\mathbf{k})\gamma^0[V(\mathbf{k},\mathbf{k}')\Phi(\mathbf{k}')]\gamma^0\Lambda_-^2(-\mathbf{k})}{M-E_1-E_2}\right. \\ &- \left.\frac{\Lambda_-^1(\mathbf{k})\gamma^0[V(\mathbf{k},\mathbf{k}')\Phi(\mathbf{k}')]\gamma^0\Lambda_+^2(-\mathbf{k})}{M+E_1+E_2}\right] . \end{aligned} \tag{1}$$

Here, $\Lambda_\pm^i$'s are the usual energy projection operators, given by

$$\Lambda_\pm^i = \frac{E_i(\mathbf{k}) \pm H_i(\mathbf{k})}{2E_i(\mathbf{k})} , \tag{2}$$

with H_i being the generalized Dirac Hamiltonians,

$$H_i(\mathbf{k}) = A_i(\mathbf{k})\boldsymbol{\alpha}\cdot\hat{\mathbf{k}} + B_i(\mathbf{k})\beta , \tag{3}$$

and $E_i(\mathbf{k}) = \sqrt{A_i(\mathbf{k})^2 + B_i(\mathbf{k})^2}$. Again, we'll consider constituent quarks of masses m_i, so that

$$A_i(\mathbf{k}) = k , \tag{4}$$

$$B_i(\mathbf{k}) = m_i , \tag{5}$$

$$E_i(\mathbf{k}) = \sqrt{m_i^2 + \mathbf{k}^2} . \tag{6}$$

The formal product of $V\Phi$ in equation (1) represents the sum of scalar potentials V_i and bilinear covariants,

$$V(\mathbf{k},\mathbf{k}')\Phi(\mathbf{k}') \longrightarrow \sum_i V_i(\mathbf{k},\mathbf{k}')G_i\Phi(\mathbf{k}')G_i , \tag{7}$$

where the G_i's are Dirac matrices.

The reduced Salpeter equation is obtained by dropping the second term from (1), and this is usually justified for heavy-quark systems on the grounds that

$$\frac{M - E_1 - E_2}{M + E_1 + E_2} \ll 1 \ . \tag{8}$$

The resulting equation,

$$M\Phi(\mathbf{k}) = (E_1 + E_2)\Phi(\mathbf{k}) + \int \frac{d^3\mathbf{k}'}{(2\pi)^3}\Lambda_+^1(\mathbf{k})\gamma^0[V(\mathbf{k},\mathbf{k}')\Phi(\mathbf{k}')]\gamma^0\Lambda_-^2(-\mathbf{k}) \ , \tag{9}$$

is a standard eigenvalue equation, and it has been used in a number of studies of relativistic bound states [8, 9, 10].

In order to apply Lagaë's formalism [2] to the reduced Salpeter equation, we multiply (9) by γ^0, and define

$$\chi(\mathbf{k}) = \Phi(\mathbf{k})\gamma^0 \ , \tag{10}$$

$$\Gamma_i = \gamma^0 G_i \ , \tag{11}$$

so that (9) becomes

$$M\chi = (E_1 + E_2)\chi + \sum_i \int \frac{d^3\mathbf{k}'}{(2\pi)^3} V_i(\mathbf{k} - \mathbf{k}')\Lambda_+^1\Gamma_i\chi'\Gamma_i\Lambda_-^2 \ , \tag{12}$$

where notation $f = f(\mathbf{k})$, $f' = f(\mathbf{k}')$ is employed. $V_i(\mathbf{k} - \mathbf{k}')$ has the Fourier transform $V(r)$ in the case of Lorentz vector kernel, and $-V(r)$ in the case of Lorentz scalar kernel.

Using properties of projection operators, it can be easily shown that the full Salpeter amplitude satisfies

$$\frac{H_1}{E_1}\chi + \chi\frac{H_2}{E_2} = 0 \ . \tag{13}$$

For the reduced equation, this constraint breaks into two parts,

$$H_1\chi = E_1\chi \ , \tag{14}$$

$$\chi H_2 = -E_2\chi \ . \tag{15}$$

Taking these constraints into account, the norm of the reduced Salpeter amplitude [11, 12, 13] can be written as

$$||\chi||^2 = \int \frac{d^3\mathbf{k}'}{(2\pi)^3} \mathrm{Tr}\left[\chi^\dagger \chi\right] \ , \tag{16}$$

and is related to the normalization of bound states as

$$||\chi||^2 = \frac{1}{(2\pi)^3}\langle B|B\rangle \ . \tag{17}$$

Using (12) inside of (16) one obtains

$$M||\chi||^2 = \int \frac{d^3\mathbf{k}}{(2\pi)^3}[E_1+E_2]\ \mathrm{Tr}[\chi^\dagger\chi] + \sum_i \int \frac{d^3\mathbf{k}}{(2\pi)^3}\int \frac{d^3\mathbf{k}'}{(2\pi)^3} V_i(\mathbf{k}-\mathbf{k}')\ \mathrm{Tr}[\chi^\dagger \Gamma_i \chi' \Gamma_i] \ . \tag{18}$$

This equation will be used for obtaining radial equations from the variational principle as outlined in [2]. It is interesting to note that it has the same form for both full and reduced Salpeter equations.

Now, in the case of the full Salpeter equation, one expands the amplitude as

$$\chi = \mathcal{L}_0 + \mathcal{L}_i\rho_i + \boldsymbol{\mathcal{N}}_0\cdot\boldsymbol{\sigma} + \boldsymbol{\mathcal{N}}_i\cdot\rho_i\boldsymbol{\sigma} \ , \tag{19}$$

with 16 Hermitian matrices whose squares are unity $(1, \rho_i, \boldsymbol{\sigma}, \rho_i\boldsymbol{\sigma})$ defined in [2]. Using this decomposition, it is easily seen that constraint (13) can be satisfied by expressing the 16 components of χ ($\mathcal{L}$'s and $\boldsymbol{\mathcal{N}}$'s) in terms of eight functions $(L_1, L_2, \mathbf{N}_1, \mathbf{N}_2)$. The correct form for $\mathcal{L}$'s and $\boldsymbol{\mathcal{N}}$'s is given in [5]. For the reduced Salpeter equation, both constraints (14) and (15) can be simultaneously satisfied if $L_1 = L_2 \equiv L$ and $\mathbf{N}_1 = \mathbf{N}_2 \equiv \mathbf{N}$.

Following [13], we obtain the radial equations by expressing L and $\mathbf{N}$ in terms of spherical harmonics and vector spherical harmonics [14], so that

$$L(\mathbf{k}) = L(k)Y_{JM}(\hat{\mathbf{k}}) \ , \tag{20}$$

$$\mathbf{N}(\mathbf{k}) = N_-(k)\mathbf{Y}_-(\hat{\mathbf{k}}) + N_0(k)\mathbf{Y}_0(\hat{\mathbf{k}}) + N_+(k)\mathbf{Y}_+(\hat{\mathbf{k}}) \ , \tag{21}$$

where $\mathbf{Y}_-$, $\mathbf{Y}_0$, and $\mathbf{Y}_+$, stand for $\mathbf{Y}_{JJ-1M}$, $\mathbf{Y}_{JJM}$, and $\mathbf{Y}_{JJ+1M}$, respectively. We also introduce functions n_+ and n_-, defined as

$$\begin{bmatrix} n_+ \\ n_- \end{bmatrix} = \begin{bmatrix} \mu & \nu \\ -\nu & \mu \end{bmatrix} \begin{bmatrix} N_+ \\ N_- \end{bmatrix}, \tag{22}$$

with

$$\mu = \sqrt{\frac{J}{2J+1}}\ ,\ \nu = \sqrt{\frac{J+1}{2J+1}}\ . \tag{23}$$

Using these definitions inside expressions for the $\mathcal{L}$'s and $\boldsymbol{\mathcal{N}}$'s as given in [5], together with properties of spherical and vector spherical harmonics, (18) can be expressed in terms of radial wave functions only. Then by taking variations with respect to $L^*(k), N_0^*(k), n_+^*(k)$, and $n_-^*(k)$, as explained in [2], one obtains the set of coupled equations for the radial wave functions of the reduced Salpeter amplitude. We summarize these equations in Appendix A for the kernels $\gamma^0 \otimes \gamma^0$, $\mathbf{1} \otimes \mathbf{1}$ and $\gamma^\mu \otimes \gamma_\mu$.

3 Numerical results

As outlined in Appendix B of [5], one can solve the system of radial equations by expanding the wave functions in terms of a complete set of basis states, which depend on a variational parameter β, and then truncating the expansion to a finite number of basis states. In this way, a set of coupled radial equations can be transformed into a matrix equation, $\mathcal{H}\psi = M\psi$. The eigenvalues M of the matrix $\mathcal{H}$ will depend on β, and by looking for the extrema of $M(\beta)$, one can find the bound state energies. If the calculation is stable, increasing the number of basis states used will decrease the dependence of the eigenvalues on β. Regions of β with the same eigenvalues should emerge and enlarge. For each of the results discussed in the remainder of this paper we have verified that this indeed occurs.

3.1 Equal mass case with $\gamma^0 \otimes \gamma^0$ kernel

In Figure 1 we compare solutions of reduced and full Salpeter equations for equal mass systems with a pure time component vector confinement ($V(r) = ar$, $a = 0.2\ GeV^2$). We have varied the quark masses ($m_1 = m_2 \equiv m$) from 0 to 1 GeV, solved both equations for all $J = 0, 1,$ and 2 states (which involves all S, P, and most D waves), and plotted the difference between state mass and rest mass of the two quarks. As one can see, the difference between the two solutions is noticeable only for $J^{PC} = 0^{-+}$ and 0^{++} states, and then only for very small quark masses. For example, for zero quark masses the difference for the 0^{-+} state is about 25 MeV, while already for quark masses of 0.3 GeV it is only 6 MeV. On the other hand, for the 1^{--} state the difference between the two solutions is about 1 MeV even for zero quark masses. Another interesting thing to observe in Figure 1 is that for both equations and for zero quark mass we have degeneracy of 0^{-+} and 0^{++}, 1^{--} and 1^{++}, and also 2^{++} and 2^{--} states. This parity degeneracy can be easily explained by referring to the radial equations for the full Salpeter equation given in Appendix A of [5]. In the limit where both masses go to zero, it can be easily seen that 0^{-+} and 0^{++} equations are the same. Similarly, for $J > 0$ states the four radial equations for $P = (-1)^J$ and $C = (-1)^J$ (involving n_{1+}, n_{2+}, n_{1-} and n_{2-}) decouple into two systems of two equations. The first one (involving n_{1+} and n_{2+}) is the same as the system describing $P = (-1)^{J+1}$ and $C = (-1)^{J+1}$ states, while the second one (involving n_{1-} and n_{2-}) is equivalent to the system describing $P = (-1)^{J+1}$ and $C = (-1)^J$ states (and higher in energy, as can be seen in Figure 1). The $m = 0$ degeneracy is an example of the chiral symmetry of the vector potential and its Wigner-Weyl realization through parity doublets.

In order to see the effects of the short range Coulomb potential, we have performed a similar analysis with $V(r) = ar - \frac{\kappa}{r}$, using $a = 0.2\ GeV^2$ and $\kappa = 0.5$. The results are shown in Figure 2. Again, the difference between full and reduced Salpeter solutions is noticeable only for the $J^{PC} = 0^{-+}$ and 0^{++} states. For the

0^{-+} state, the difference is now about 35 MeV for $m_1 = m_2 = m = 0$, and about 10 MeV for $m_1 = m_2 = m = 0.3\ GeV$. For the 1^{--} state, the difference is only about 3 MeV for zero quark masses.

Finally, in Figure 3 we show the results of the same analysis as above, but this time including an additive constant, $V(r) = ar + C - \frac{\kappa}{r}$ ($a = 0.2\ GeV^2$, $C = -1.0\ GeV$, and $\kappa = 0.5$). One might expect that adding a constant to the potential would not change the difference between the two equations. However, as one can see from the Figure 3, it is not quite like that. Now the solutions to the full Salpeter equation for the 0^{-+} and 0^{++} states are considerably lower in energy than the solutions to the reduced Salpeter equation. For the 0^{-+} (1^{--}) state the difference is about 106 MeV (7 MeV) with zero quark masses and about 3 MeV (1 MeV) with $m_1 = m_2 = 1.0\ GeV$.

The reason for this somewhat unexpected behavior is that a negative constant C added to the kernel of the full Salpeter equation lowers the eigenvalues by an amount larger than $|C|$, while for the reduced Salpeter equation it is exactly $|C|$. For example, adding $C = -1.0\ GeV$ to the potential $V(r) = ar - \frac{\kappa}{r}$ with $a = 0.2\ GeV^2$ and $\kappa = 0.5$ the lowest eigenvalue for the 0^{-+} state (with zero quark masses) is lowered by about 1.072 GeV for the full Salpeter equation with a time component vector kernel. This effect is much less noticeable with larger quark masses, and higher J states, e.g. for the 1^{--} state with zero quark masses and same a and κ as before, the lowest eigenvalue was lowered by 1.004 GeV after adding $C = -1.0\ GeV$. We also note that these numerical results were obtained with 25 basis states, so that dependence of the results on the variational parameter characterizing the basis states was negligible.

In order to further explore the relationship between the full Salpeter equation and the reduced one, we have plotted the radial wave functions for the 0^{-+} case and for $V(r) = ar + C - \frac{\kappa}{r}$ ($a = 0.2\ GeV^2$, $C = -1.0\ GeV$, and $\kappa = 0.5$). Just as a reminder, the reduced Salpeter equation for the pseudoscalar case has only one wave

function (L), as opposed to two (L_1 and L_2) in the full equation. Also, when the reduced Salpeter equation is valid, then L_1 and L_2 are equal. As we can see from Figure 4, for very small quark masses ($m_1 = m_2 = 0$), the difference between L_1 and L_2 is large, and the reduced equation cannot replace the full one. However, with $m_1 = m_2 = 1.0\ GeV$ (Figure 5), the reduced Salpeter result is much more closer to the full one. In these two figures we use a Cornell potential with an additive constant ($a = 0.2\ GeV^2,\ C = -1.0\ GeV$, and $\kappa = 0.5$).

From this analysis, it is clear that the solutions of the reduced Salpeter equation are nearly the same as those of the full one for the description of the heavy-heavy ($c\bar{c}$ and $b\bar{b}$) mesons, and a very good first approximation even for the $s\bar{s}$ mesons (with s quark mass of about 500 MeV). This justifies the assumption of Gara et. al. [10] that the reduced Salpeter equation could be used for the description of $s\bar{s}$ mesons.

3.2 Heavy-light case with $\gamma^0 \otimes \gamma^0$ kernel

A similar analysis can be performed for the "heavy-light" systems. For $V(r) = ar + C - \frac{\kappa}{r}$, with $a = 0.2\ GeV^2$, $C = -1.0\ GeV$, and $\kappa = 0.5$, we fixed the "light" quark mass at $m_1 = 0$, varied the "heavy" antiquark mass m_2 from 0 to 1 GeV, and solved both equations for all $J = 0, 1$ and 2 states. The results are shown in Figure 6. The degeneracy of states with the same J and different parity can be again explained easily by looking into the radial equations for the full Salpeter equation given in Appendix A of [5]. In the limit where $m_1 \to 0$, $\phi_1 \to 0$ and $\phi \to \theta$, which makes equivalent the two sets of equations for different parities. As far as the difference between the full and reduced Salpeter equations are concerned, it is again important only for $J = 0$ states. For example, for 0^- and 0^+ (1^- and 1^+) it is only about 7 MeV (1 MeV) at $m_2 = 1.0\ GeV$. Figure 7 shows that for $m_1 = 0,\ m_2 = 1\ GeV$, L is already a very good approximation to L_1 and L_2. One also has to remember that with such a large negative constant the c quark mass must be considerably larger than 1.0 GeV in order to describe D mesons. Given all

this, we conclude that the reduced Salpeter equation is an excellent approximation to the full one for the description of D and B mesons.

Although the time component vector interaction has many nice properties, it is flawed as a realistic quark confinement interaction. As pointed out earlier, it predicts "parity doubling" of meson states in the limit of zero quark mass. For large quark masses this difficulty appears as the "wrong sign" spin-orbit interaction which conflicts both with experiment and QCD.

3.3 Mixed confinement potentials

As already mentioned, recently a half-half mixture of the time component vector and scalar confinement has been proposed in [3], together with a one gluon exchange kernel, for the investigation of weak decays of B and D mesons. In order to compare the full Salpeter equation with its reduced version in this type of model, we adopt the mixed confining kernel,

$$\frac{1}{2}[\gamma^0 \otimes \gamma^0 + \mathbf{1} \otimes \mathbf{1}]V_c(r) \ , \tag{24}$$

with

$$V_c(r) = ar + C \ , \tag{25}$$

and for the short range potential we simply take

$$[\gamma^0 \otimes \gamma^0]V_g(r) \ , \tag{26}$$

where

$$V_g(r) = -\frac{\kappa}{r} \ . \tag{27}$$

A confinement mixture of this type has been shown to have a stable variational solution [5]. For the parameters of the potential we choose $a = 0.2\ GeV^2$, $C = -1.0\ GeV$, and $\kappa = 0.5$. Computation of the equal mass case is shown in Figure 8 (for the 0^{-+} and 0^{++} states). As one can see, the differences between full and

reduced Salpeter solutions are only slightly different than in the case with a pure time component vector kernel. For the 0^{-+} state and $m_1 = m_2 = m = 1.0\ GeV$ the difference between the two equations is about 7 MeV. The heavy-light case calculation (for the same potential parameters) is shown in Figure 9. The difference between the two solutions for the 0^- state, and for $m_1 = 0$ and $m_2 = 1.0\ GeV$, is about 9 MeV. Therefore, we again conclude that the reduced Salpeter equation is as good as the full Salpeter equation for the description of the $c\bar{c}$ and $b\bar{b}$ mesons, a very good first approximation even for the $s\bar{s}$ mesons, and would serve as well as the full Salpeter equation for the description of the heavy-light systems, such as D and B mesons.

Of course, these results are dependent on parameters of the particular model. However, in our analysis we have used values for a and κ that are typical in the hadron spectroscopy, and constant C that is perhaps slightly larger than usual. We have also restricted ourselves to constituent masses that are smaller than the usually assumed c quark mass. Therefore, we feel that our main conclusions would not be drastically altered if a different set of realistic parameters was used.

In order to illustrate this, we have chosen parameters of the potential to be as close as possible to the ones used in [3] (as given in their Table 1), i.e. $m_1 = 0.2\,GeV$, $m_2 = 1.738\ GeV$, $a = 0.335\ GeV^2$, $C = -1.027\ GeV$, and $\kappa = 0.521$ (which corresponds to $\alpha_{sat} = 0.391$ in [3]), and solved both equations for the 0^- and 0^+ states, with the kernel described by (24-27). The differences between ground state energies were 5 MeV and 0 MeV, respectively, despite the large value of a. For the 0^- state, where the difference between the two solutions should be most obvious, we have plotted the radial wave functions in Figure 10. As one can see, the reduced wave function is a very good approximation for the full wave functions.

For the sake of simplicity, in the previous calculations we have used a short range potential with a fixed coupling constant, for which Murota [12] has shown most of the Salpeter amplitudes are divergent as $r \to 0$. If one uses a running coupling

constant, this divergence is less pronounced, but still present. That is precisely the reason why the short range potential used in [3] was regularized. In order to show the effects of regularization, instead of (27) we now take as in [3]

$$V_g(r) = \begin{cases} -\frac{4}{3}\frac{\alpha(r)}{r} \ , & r \geq r_0 \\ a_g r^2 + b_g \ , & r < r_0 \end{cases} \ . \tag{28}$$

The constants a_g and b_g are determined by the condition that $V_g(r)$ and its derivative are continuous functions. The running coupling constant is parametrized exactly as in [3], with their value of $r_0 = 0.507\ GeV^{-1}$, and the saturation value for the coupling constant $\alpha_{sat} = 0.391$. The string tension and constant were again $a = 0.335\ GeV^2$ and $C = -1.027\ GeV$, and quark masses were $m_1 = 0.2\ GeV$ and $m_2 = 1.738\ GeV$, as for the previous calculation. Using these parameters, we have again solved both equations for the 0^- and 0^+ states. The differences between ground state energies were $3\ MeV$ and $0\ MeV$, respectively, showing that a regularized short range potential reduces the differences between the reduced and the full Salpeter equation. For the 0^- state, we have again plotted the radial wave functions in Figure 11. As one can see, all wave functions are now finite at the origin, and the reduced Salpeter wave function is an even better approximation to the full ones than it was before.

We can also use this model to estimate the accuracy of $\frac{1}{m}$ recoil corrections to the heavy-light limit. In Figure 12 we show the difference between the 0^- ground states for a finite and an infinite heavy mass (m_2) with a massless light quark (m_1) in both cases. We see that these "recoil" corrections are quite important even for the b quark mesons where correction is nearly 40 MeV (at $\frac{1}{m_2} \simeq 0.2\ GeV^{-1}$). On the other hand, the difference between full and reduced Salpeter solutions is small. For a charmed meson ($\frac{1}{m_2} \simeq 0.66\ GeV^{-1}$) the difference is about 3.5 MeV, while for a meson with a b quark it is about 0.2 MeV.

In [3] the mixed confinement (24) was used in part because the full Salpeter equation does not have stable solutions unless the scalar confinement part is equal

or less than the time component vector part. We should note that the pure scalar confinement could have been used with the reduced Salpeter equation.

4 Conclusions

The reduced Salpeter equation, also known as the no-pair equation, has long been used in dynamical models of mesons. It has also been long appreciated that it is an approximation to the full Salpeter equation and that the discarded portion only vanishes if at least one of the constituent masses is infinite. The reduced equation has nevertheless been used because it has the standard hermitian form.

In this paper we have examined the conditions under which the reduced equation can be employed without significant loss in accuracy. The critical factors turn out to be constituent mass, J^P state, and the nature of the interaction. If the total quark mass exceeds about 1.0 GeV very little difference is found between the full and reduced Salpeter solutions. Also, with the exception of the 0^- and 0^+ states very little difference is found even at zero quark mass. Finally, even for $0^\pm$ states and vanishing quark mass the differences between full and reduced Salpeter solutions are small if there is no large constant in the coordinate space confining potential.

There remain a number of hadronic states with light quark masses in which the full Salpeter equation must be used. Differences up to 100 MeV were found between pseudoscalar masses at zero quark mass for the two equations.

In our comparison between the full and reduced Salpeter solutions we have considered both energies and wave functions. As was the case with the energy eigenvalues, we see large differences between the 0^- full and reduced wave functions for zero quark mass (see Fig. 4). The differences are largest at the origin, $r = 0$. As observed in subsequent figures, increasing the quark mass and considering higher states causes the reduced Salpeter wave functions to become more similar to the full ones. The difference between the two solutions is always most noticeable at the

origin.

We have primarily considered the time component vector kernel, since its solutions with the full Salpeter equation are variationally stable and yield normal linear Regge trajectories in the case of linear confinement [5]. Although the solutions with a time component vector potential have many desirable properties, a quark confinement of this type has a spin-orbit interaction of the wrong sign. The addition of up to equal parts Lorentz scalar confinement has been advocated recently [3] for the study of weak decays of heavy-light mesons. The variational stability is retained in this case and the reduced Salpeter equation is shown to be accurate under similar conditions as in the pure time component vector case. The reduced equation has the additional advantage of variational stability with pure scalar confinement.

APPENDIX

A Radial equations

In this appendix we give the final form of the radial equations for the reduced Salpeter equation for the kernels $\gamma^0 \otimes \gamma^0$, $\mathbf{1} \otimes \mathbf{1}$ and $\gamma^\mu \otimes \gamma_\mu$. These equations represent a general case with a quark of mass m_1 and an anti-quark of mass m_2. However, one has to keep in mind that for $J = 0$ two wave functions vanish, i.e. we have $N_0 = 0$, and $n_+ = 0$.

As in [5, 2] we have used notation

$$S_\phi = \sin\phi \ , \ C_\phi = \cos\phi \ , \tag{29}$$

$$S_\theta = \sin\theta \ , \ C_\theta = \cos\theta \ , \tag{30}$$

with angles ϕ and θ defined as

$$\phi = \frac{\phi_1 + \phi_2}{2} \ , \ \theta = \frac{\phi_2 - \phi_1}{2} \ , \tag{31}$$

while ϕ_i's are defined through

$$\cos\phi_i = \frac{A_i}{E_i} \ , \ \sin\phi_i = \frac{B_i}{E_i} \ . \tag{32}$$

A_i, B_i and E_i are defined in (4-6).

In the equal mass case the equations given below somewhat simplify, since one has $E_1 = E_2$, $\phi = \phi_1 = \phi_2$, and $\theta = 0$, so that $S_\theta = 0$ and $C_\theta = 1$. Also, since charge conjugation is a good quantum number in the equal mass case, the two $P = (-1)^{J+1}$ state equations decouple into two separate equations, one corresponding to $C = (-1)^J$ (involving L), and the other corresponding to $C = (-1)^{J+1}$ (involving N_0).

The heavy-light limit ($m_2 \to \infty$) is obtained by setting $E_2 \to m_2$, $\phi_2 \to \frac{\pi}{2}$, so that $S_\theta \to C_\phi$ and $C_\theta \to S_\phi$. As expected, in the heavy-light limit equations for the

$\gamma^0 \otimes \gamma^0$ and $\gamma^\mu \otimes \gamma_\mu$ kernels are the same. Also, in this case spin of the heavy quark decouples from the spin of the light quark, so that total angular momentum j of the light quark becomes a good quantum number. Inverting (22),

$$N_+ = \mu n_+ - \nu n_- \ , \tag{33}$$

$$N_- = \nu n_+ + \mu n_- \ , \tag{34}$$

and also putting

$$L_+ = \nu L - \mu N_0 \ , \tag{35}$$

$$L_- = \mu L + \nu N_0 \ , \tag{36}$$

from the heavy-light limit equations in terms of n_+, n_-, N_0 and L, one can obtain decoupled equations in terms of N_+, N_-, L_+ and L_-, describing heavy-light states with quantum number j. There will always be a pair of degenerate states, described with N_- and L_+ ($J = L + 1$ and $J = L$, for the state with $j = L + \frac{1}{2}$), and N_+ and L_- ($J = L - 1$ and $J = L$, for the state with with $j = L - \frac{1}{2}$).

For any mixture of different kernels, only the kernel parts of the radial equations should be added. The kinetic energy terms are always the same. In the $\mathbf{1} \otimes \mathbf{1}$ case, we have introduced an additional minus sign in the kernel, so that $V(r)$ has the same form for all three cases considered, e.g. for the Cornell potential $V(r) = ar - \frac{\kappa}{r}$.

A.1 $\gamma^0 \otimes \gamma^0$ kernel

States with parity $P = (-1)^{J+1}$:

$$\begin{aligned} ML &= [E_1 + E_2]L + \frac{1}{2}\int_0^\infty \frac{k'^2 dk'}{(2\pi)^2}[C_\theta V_J C'_\theta L' + S_\phi V_J S'_\phi L' \\ &+ S_\theta(\mu^2 V_{J-1} + \nu^2 V_{J+1}) S'_\theta L' + C_\phi(\mu^2 V_{J-1} + \nu^2 V_{J+1}) C'_\phi L' \\ &+ \mu\nu S_\theta(V_{J-1} - V_{J+1}) C'_\phi N'_0 + \mu\nu C_\phi(V_{J-1} - V_{J+1}) S'_\theta N'_0] \ , \\ MN_0 &= [E_1 + E_2]N_0 + \frac{1}{2}\int_0^\infty \frac{k'^2 dk'}{(2\pi)^2}[C_\theta V_J C'_\theta N'_0 + S_\phi V_J S'_\phi N'_0 \end{aligned} \tag{37}$$

$$
\begin{aligned}
&+ \quad C_\phi(\nu^2 V_{J-1} + \mu^2 V_{J+1}) C'_\phi N'_0 + S_\theta(\nu^2 V_{J-1} + \mu^2 V_{J+1}) S'_\theta N'_0 \\
&+ \quad \mu\nu C_\phi (V_{J-1} - V_{J+1}) S'_\theta L' + \mu\nu S_\theta (V_{J-1} - V_{J+1}) C'_\phi L'] \ .
\end{aligned}
$$

States with parity $P = (-1)^J$:

$$
\begin{aligned}
Mn_+ &= [E_1 + E_2] n_+ + \frac{1}{2} \int_0^\infty \frac{k'^2 dk'}{(2\pi)^2} [C_\phi V_J C'_\phi n'_+ + S_\theta V_J S'_\theta n'_+ \\
&+ \quad S_\phi(\nu^2 V_{J-1} + \mu^2 V_{J+1}) S'_\phi n'_+ + C_\theta(\nu^2 V_{J-1} + \mu^2 V_{J+1}) C'_\theta n'_+ \\
&+ \quad \mu\nu S_\phi (V_{J-1} - V_{J+1}) C'_\theta n'_- + \mu\nu C_\theta (V_{J-1} - V_{J+1}) S'_\phi n'_-] \ , \qquad (38) \\
Mn_- &= [E_1 + E_2] n_- + \frac{1}{2} \int_0^\infty \frac{k'^2 dk'}{(2\pi)^2} [C_\phi V_J C'_\phi n'_- + S_\theta V_J S'_\theta n'_- \\
&+ \quad C_\theta(\mu^2 V_{J-1} + \nu^2 V_{J+1}) C'_\theta n'_- + S_\phi(\mu^2 V_{J-1} + \nu^2 V_{J+1}) S'_\phi n'_- \\
&+ \quad \mu\nu C_\theta (V_{J-1} - V_{J+1}) S'_\phi n'_+ + \mu\nu S_\phi (V_{J-1} - V_{J+1}) C'_\theta n'_+] \ .
\end{aligned}
$$

A.2 $\mathbf{1 \otimes 1}$ kernel

States with parity $P = (-1)^{J+1}$:

$$
\begin{aligned}
ML &= [E_1 + E_2] L + \frac{1}{2} \int_0^\infty \frac{k'^2 dk'}{(2\pi)^2} [C_\theta V_J C'_\theta L' + S_\phi V_J S'_\phi L' \\
&- \quad S_\theta(\mu^2 V_{J-1} + \nu^2 V_{J+1}) S'_\theta L' - C_\phi(\mu^2 V_{J-1} + \nu^2 V_{J+1}) C'_\phi L' \\
&- \quad \mu\nu S_\theta (V_{J-1} - V_{J+1}) C'_\phi N'_0 - \mu\nu C_\phi (V_{J-1} - V_{J+1}) S'_\theta N'_0] \ , \qquad (39) \\
MN_0 &= [E_1 + E_2] N_0 + \frac{1}{2} \int_0^\infty \frac{k'^2 dk'}{(2\pi)^2} [C_\theta V_J C'_\theta N'_0 + S_\phi V_J S'_\phi N'_0 \\
&- \quad C_\phi(\nu^2 V_{J-1} + \mu^2 V_{J+1}) C'_\phi N'_0 - S_\theta(\nu^2 V_{J-1} + \mu^2 V_{J+1}) S'_\theta N'_0 \\
&- \quad \mu\nu C_\phi (V_{J-1} - V_{J+1}) S'_\theta L'] - \mu\nu S_\theta (V_{J-1} - V_{J+1}) C'_\phi L'] \ .
\end{aligned}
$$

States with parity $P = (-1)^J$:

$$
\begin{aligned}
Mn_+ &= [E_1 + E_2] n_+ + \frac{1}{2} \int_0^\infty \frac{k'^2 dk'}{(2\pi)^2} [-C_\phi V_J C'_\phi n'_+ - S_\theta V_J S'_\theta n'_+ \\
&+ \quad S_\phi(\nu^2 V_{J-1} + \mu^2 V_{J+1}) S'_\phi n'_+ + C_\theta(\nu^2 V_{J-1} + \mu^2 V_{J+1}) C'_\theta n'_+
\end{aligned}
$$

$$
\begin{aligned}
&+ \quad \mu\nu S_\phi (V_{J-1} - V_{J+1}) C'_\theta n'_- + \mu\nu C_\theta (V_{J-1} - V_{J+1}) S'_\phi n'_-] \ , \qquad (40)\\
Mn_- &= [E_1 + E_2] n_- + \frac{1}{2} \int_0^\infty \frac{k'^2 dk'}{(2\pi)^2} [-C_\phi V_J C'_\phi n'_- - S_\theta V_J S'_\theta n'_-\\
&+ \quad C_\theta (\mu^2 V_{J-1} + \nu^2 V_{J+1}) C'_\theta n'_- + S_\phi (\mu^2 V_{J-1} + \nu^2 V_{J+1}) S'_\phi n'_-\\
&+ \quad \mu\nu C_\theta (V_{J-1} - V_{J+1}) S'_\phi n'_+ + \mu\nu S_\phi (V_{J-1} - V_{J+1}) C'_\theta n'_+] \ .
\end{aligned}
$$

A.3 $\gamma^\mu \otimes \gamma_\mu$ kernel

States with parity $P = (-1)^{J+1}$:

$$
\begin{aligned}
ML &= [E_1 + E_2] L + \int_0^\infty \frac{k'^2 dk'}{(2\pi)^2} [2 C_\theta V_J C'_\theta L' - S_\phi V_J S'_\phi L'\\
&+ \quad S_\theta (\mu^2 V_{J-1} + \nu^2 V_{J+1}) S'_\theta L' + \mu\nu S_\theta (V_{J-1} - V_{J+1}) C'_\phi N'_0 \ , \qquad (41)\\
MN_0 &= [E_1 + E_2] N_0 + \int_0^\infty \frac{k'^2 dk'}{(2\pi)^2} [C_\theta V_J C'_\theta N'_0\\
&+ \quad C_\phi (\nu^2 V_{J-1} + \mu^2 V_{J+1}) C'_\phi N'_0 + \mu\nu C_\phi (V_{J-1} - V_{J+1}) S'_\theta L'] \ .
\end{aligned}
$$

States with parity $P = (-1)^J$:

$$
\begin{aligned}
Mn_+ &= [E_1 + E_2] n_+ + \int_0^\infty \frac{k'^2 dk'}{(2\pi)^2} [C_\phi V_J C'_\phi n'_+\\
&+ \quad C_\theta (\nu^2 V_{J-1} + \mu^2 V_{J+1}) C'_\theta n'_+ + \mu\nu C_\theta (V_{J-1} - V_{J+1}) S'_\phi n'_-] \ , \qquad (42)\\
Mn_- &= [E_1 + E_2] n_- + \int_0^\infty \frac{k'^2 dk'}{(2\pi)^2} [2 C_\phi V_J C'_\phi n'_- - S_\theta V_J S'_\theta n'_-\\
&+ \quad S_\phi (\mu^2 V_{J-1} + \nu^2 V_{J+1}) S'_\phi n'_- + \mu\nu S_\phi (V_{J-1} - V_{J+1}) C'_\theta n'_+] \ .
\end{aligned}
$$

ACKNOWLEDGMENTS

This work was supported in part by the U.S. Department of Energy under Contract Nos. DE-FG02-95ER40896 and DE-AC05-84ER40150, the National Science Foundation under Grant No. HRD9154080, and in part by the University of Wisconsin Research Committee with funds granted by the Wisconsin Alumni Research Foundation.

References

[1] E. E. Salpeter, Phys. Rev. **87**, 328 (1952).

[2] J.-F. Lagaë, Phys. Rev. D **45**, 305 (1992).

[3] G. Zöller, S. Hainzl, C. R. Münz, and M. Beyer, *Weak Decays of Heavy Mesons in the Instantaneous Bethe-Salpeter approach*, Bonn University preprint BONN-TK-94-15 (hep-ph/9412355).

[4] J. Parramore and J. Piekarewicz, Nucl. Phys. A **585**, 705 (1995).

[5] M. G. Olsson, S. Veseli, and K. Williams, *On the instantaneous Bethe-Salpeter equation*, UW-Madison preprint, MADPH-95-880 (hep-ph/9503477), Phys. Rev. D (in press).

[6] J. Sucher, Int. J. Quantum Chem. **25**, 3 (1984); G. Hardekopf and J. Sucher, Phys. Rev. A **30**, 703 (1984); Phys. Rev A **31**, 2020 (1985).

[7] J.-F. Lagaë, Phys. Rev. D **45**, 317 (1992).

[8] Vu K. Cung, T. Fulton, W. W. Repko, A. Schaum, and A. Devoto, Ann. Phys. **98**, 516 (1976).

[9] S. Jacobs, M. G. Olsson, and C. J. Suchyta III, Phys. Rev. D **33**, 3338 (1986); Phys. Rev. D **34**, 3536(E) (1986).

[10] A. Gara, B. Durand, L. Durand, and L. J. Nickisch, Phys. Rev. D **40**, 843 (1989); A. Gara, B. Durand, and L. Durand, Phys. Rev. D **42**, 1651 (1990).

[11] C. H. Llewellyn Smith, Ann. Phys. **53**, 521 (1969).

[12] T. Murota, Prog. Th. Phys. **69**, 181 (1983).

[13] A. Le Yaouanc, L. Oliver, S. Ono, O. Pène, and J.-C. Raynal, Phys. Rev. D **31**, 137 (1985).

[14] For the extensive discussion of generic wave functions and identification of the quantum numbers of the bound states the reader is again referred to [2].

FIGURES

Figure 1: Equal mass comparison of the reduced (dashed lines) and full Salpeter (full lines) equations for the time component vector kernel with $V(r) = ar$ ($a = 0.2\ GeV^2$). The energies of all states with J equal to 0, 1, and 2 are shown as a function of the quark mass. We have used 15 basis states.

Figure 2: Equal mass comparison of solutions to the reduced (dashed lines) and full Salpeter (full lines) equations for the time component vector kernel with $V(r) = ar - \frac{\kappa}{r}$ ($a = 0.2\ GeV^2, \kappa = 0.5$). The energies of all states with J equal to 0, 1, and 2 are shown as a function of the quark mass. We have used 15 basis states.

Figure 3: Equal mass comparison of the reduced (dashed lines) and full Salpeter (full lines) equations for the time component vector kernel with $V(r) = ar + C - \frac{\kappa}{r}$ ($a = 0.2\ GeV^2$, $C = -1.0\ GeV$, $\kappa = 0.5$). The energies of all states with J equal to 0, 1, and 2 are shown as a function of the quark mass. We have used 15 basis states.

Figure 4: Pseudoscalar ($J^{PC} = 0^{-+}$) radial wave functions in coordinate space for the reduced (L, dashed line) and full Salpeter equations (L_1, lower full line, and L_2, upper full line), with time component vector kernel and $V(r) = ar + C - \frac{\kappa}{r}$ ($a = 0.2\ GeV^2$, $C = -1.0\ GeV$, $\kappa = 0.5$). The quark masses were $m_1 = m_2 = 0$, and the calculation was done with 25 basis states.

Figure 5: Pseudoscalar ($J^{PC} = 0^{-+}$) radial wave functions in coordinate space for the reduced (L, dashed line) and full Salpeter equations (L_1, lower full line, and L_2, upper full line), with time component vector kernel and $V(r) = ar + C - \frac{\kappa}{r}$ ($a = 0.2\ GeV^2$, $C = -1.0\ GeV$, $\kappa = 0.5$). The quark masses $m_1 = m_2 = 1\ GeV$, and the calculation was done with 25 basis states.

Figure 6: Comparison for heavy-light mesons of the reduced (dashed lines) and full Salpeter (full lines) solutions for the time component vector kernel with $V(r) = ar + C - \frac{\kappa}{r}$ ($a = 0.2\ GeV^2$, $C = -1.0\ GeV$, $\kappa = 0.5$). The lighter quark mass was fixed at $m_1 = 0$, and we show the light degree of freedom energy $M - m_2$ as a function of m_2 for the lowest angular momentum states J^P. We have used 15 basis states.

Figure 7: Heavy-light pseudoscalar ($J^P = 0^-$) radial wave functions in coordinate space for the reduced (L, dashed line) and full Salpeter equations (L_1, lower full line, and L_2, upper full line), with time component vector kernel and $V(r) = ar + C - \frac{\kappa}{r}$ ($a = 0.2\ GeV^2$, $C = -1.0\ GeV$, $\kappa = 0.5$). The quark masses were $m_1 = 0$ and $m_2 = 1\ GeV$. The calculation was done with 25 basis states.

Figure 8: Equal mass comparison of the reduced (dashed lines) and full Salpeter (full lines) ground state 0^{-+} and 0^{++} energies. An equal mixture of the time component vector and scalar confinement ($V_c(r) = ar + C$), together with time component vector short range potential ($V_g(r) = -\frac{\kappa}{r}$) was used. The potential parameters were $a = 0.2\ GeV^2$, $C = -1.0\ GeV$, and $\kappa = 0.5$. Comparison with Figure 3 shows the breaking of the parity degeneracy at $m = 0$. 15 basis states was used for calculation.

Figure 9: Heavy-light mixed confinement comparison of the reduced (dashed lines) and full Salpeter (full lines) ground state 0^- and 0^+ energies. An equal mixture of the time component vector and scalar confinement ($V_c(r) = ar + C$), together with time component vector short range potential ($V_g(r) = -\frac{\kappa}{r}$) was used. The potential parameters were $a = 0.2\ GeV^2$, $C = -1.0\ GeV$, and $\kappa = 0.5$, while the lighter constituent mass was fixed at $m_1 = 0$. By comparing with Figure 6 we observe the lifting of the parity degeneracy present in a pure time component vector interaction at $m = 0$. 15 basis states was used in the calculation.

Figure 10: Pseudoscalar ($J^P = 0^-$) radial wave functions in coordinate space for the reduced (L, dashed line) and full Salpeter equations (L_1, lower full line, and L_2, upper full line), with a half-half mixture of the time component vector and scalar confinement ($V_c(r) = ar + C$), together with time component vector short range potential ($V_g(r) = -\frac{\kappa}{r}$). The potential parameters were $a = 0.335\ GeV^2$, $C = -1.027\ GeV$, and $\kappa = 0.521$, while the quark masses were $m_1 = 0.2$ and $m_2 = 1.738\ GeV$. The calculation was done with 25 basis states, and represents a model of [3], but with a singular short range potential.

Figure 11: Pseudoscalar ($J^P = 0^-$) radial wave functions in coordinate space for the reduced (L, dashed line) and full Salpeter equations (L_1, lower full line, and L_2, upper full line), with a half-half mixture of the time component vector and scalar confinement ($V_c(r) = ar + C$), together with the regularized time component vector short range potential (as defined in (28) in the text). The potential parameters were $a = 0.335\ GeV^2$, $C = -1.027\ GeV$, $\alpha_{sat} = 0.391$, and $r_0 = 0.507\ GeV^{-1}$, while quark masses were $m_1 = 0.2$ and $m_2 = 1.738\ GeV$. The calculation was done with 25 basis states, and represents a model of [3], including a regularized short range potential.

Figure 12: $\frac{1}{m}$ corrections to the heavy-light 0^- ground state energy as a function of $\frac{1}{m_2}$ using the model of [3], with light quark mass $m_1 = 0$, and potential parameters the same as before. The correction ranges from about 40 MeV for the B meson to about 100 MeV for the D meson. The difference between the full and reduced solutions is 0.2 MeV and 3.5 MeV for the B and D mesons respectively.

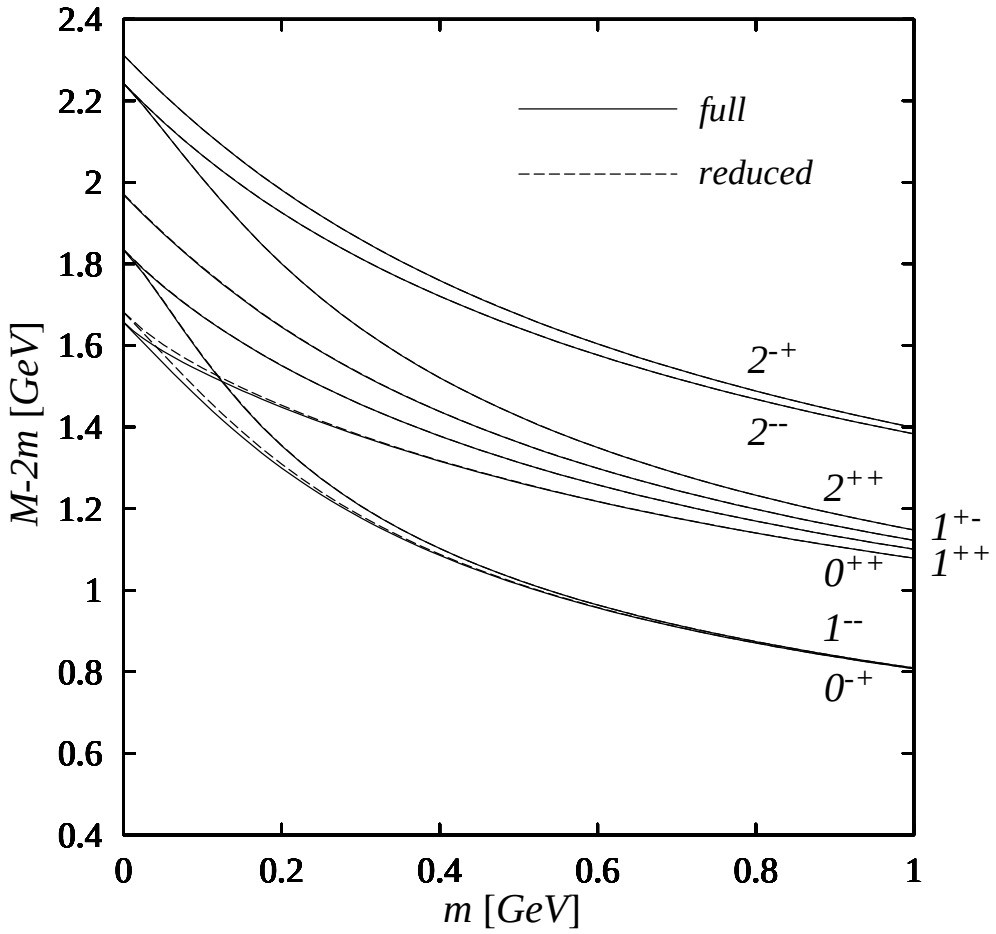
full
reduced
2^-+
2^--
2^++
1^+-
1^++
0^++
1^--
0^-+
M-2m [GeV]
m [GeV]
2.4
2.2
2
1.8
1.6
1.4
1.2
1
0.8
0.6
0.4
0
0.2
0.4
0.6
0.8
1

Figure 1

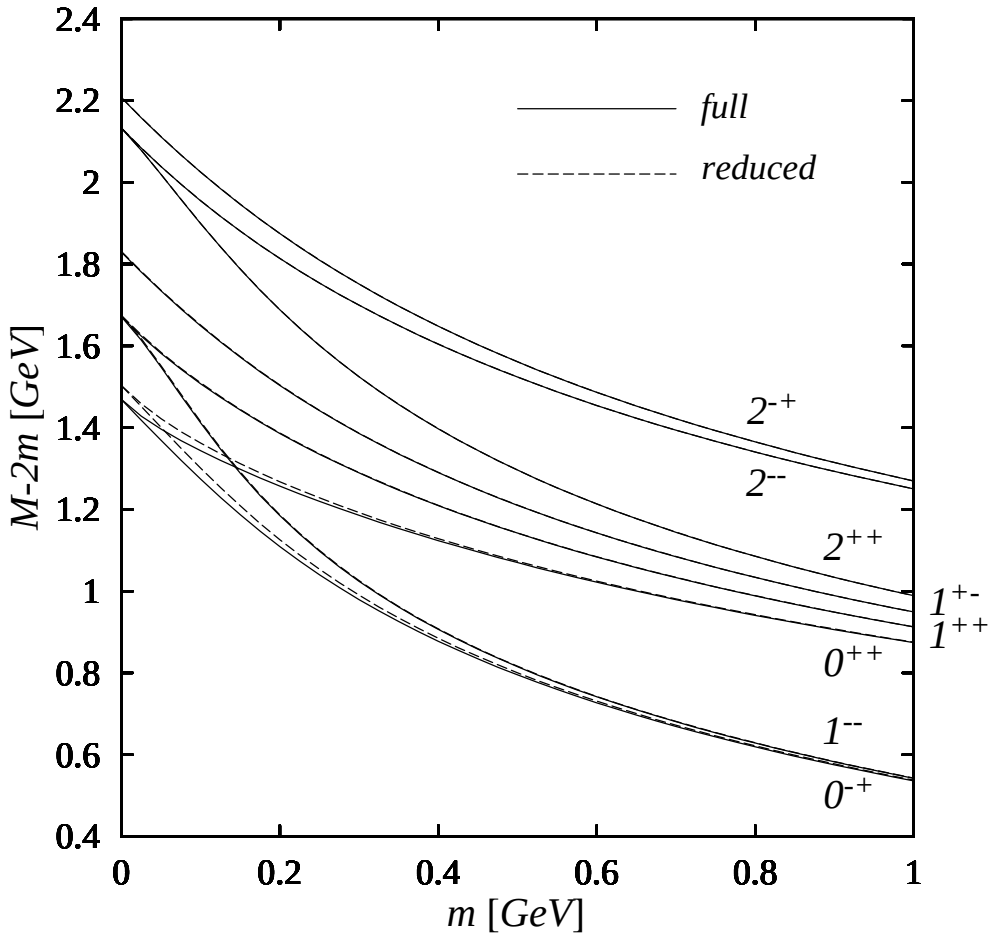
full
reduced
M-2m [GeV]
m [GeV]
2.4
2.2
2
1.8
1.6
1.4
1.2
1
0.8
0.6
0.4
0
0.2
0.4
0.6
0.8
1
2-+
2--
2++
1+-
1++
0++
1--
0-+

Figure 2

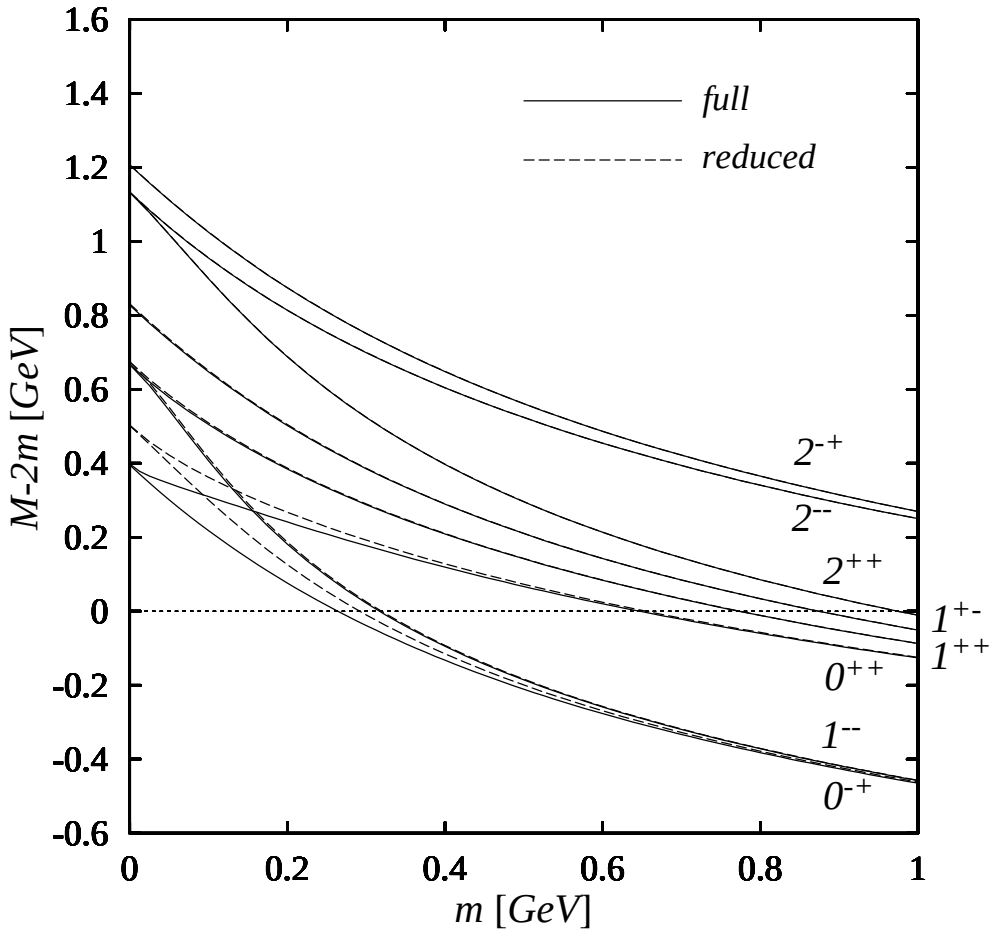
full
reduced
M-2m [GeV]
m [GeV]
2^-+
2^--
2^++
1^+-
1^++
0^++
1^--
0^-+
1.6
1.4
1.2
1
0.8
0.6
0.4
0.2
0
-0.2
-0.4
-0.6
0
0.2
0.4
0.6
0.8
1

Figure 3

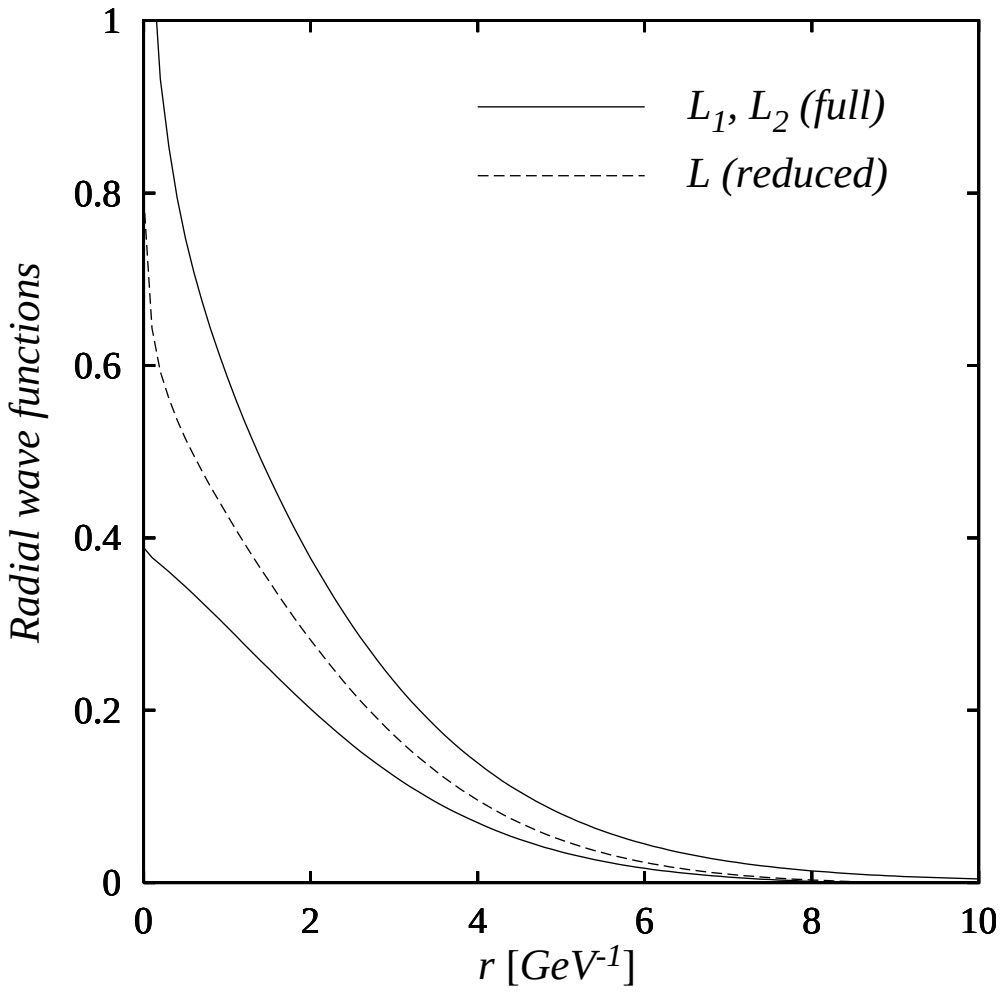
1
0.8
0.6
0.4
0.2
0
0
2
4
6
8
10
Radial wave functions
r [GeV-1]
L1, L2 (full)
L (reduced)

Figure 4

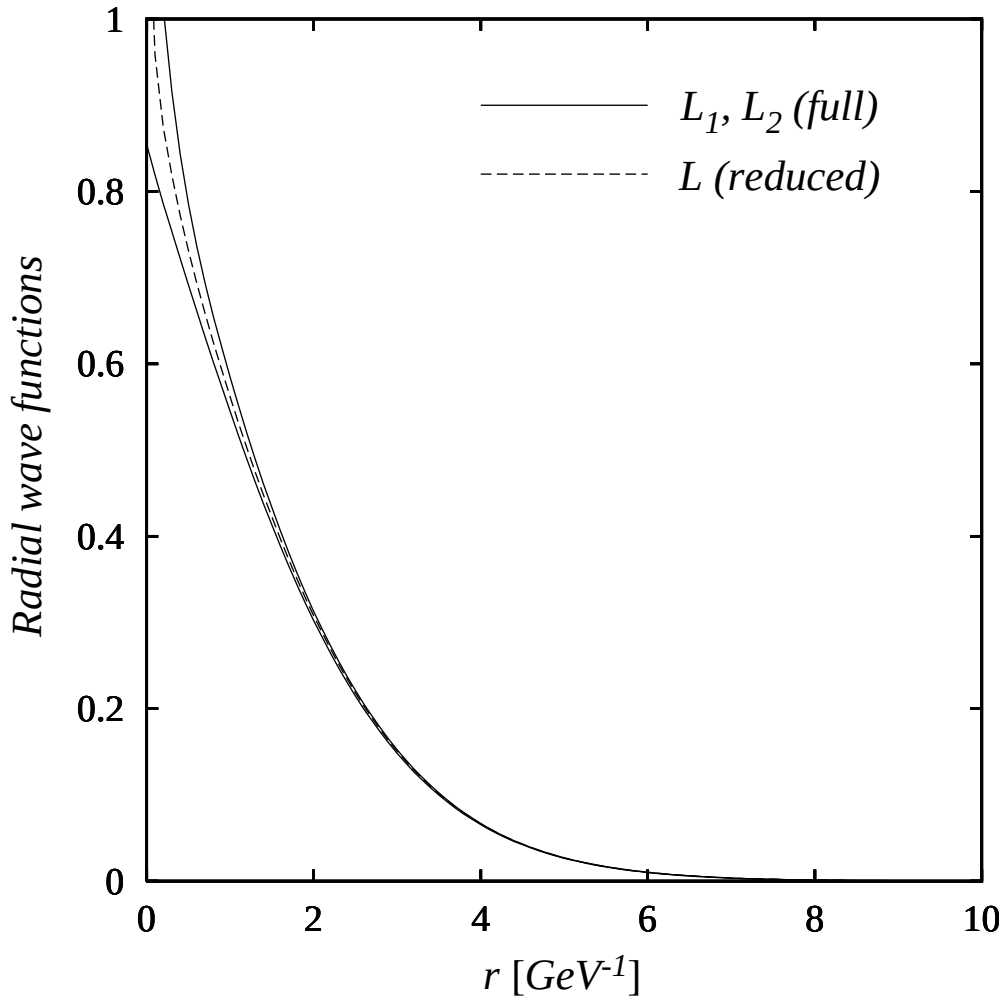
1
0.8
0.6
0.4
0.2
0
0
2
4
6
8
10
Radial wave functions
r [GeV-1]
L1, L2 (full)
L (reduced)

Figure 5

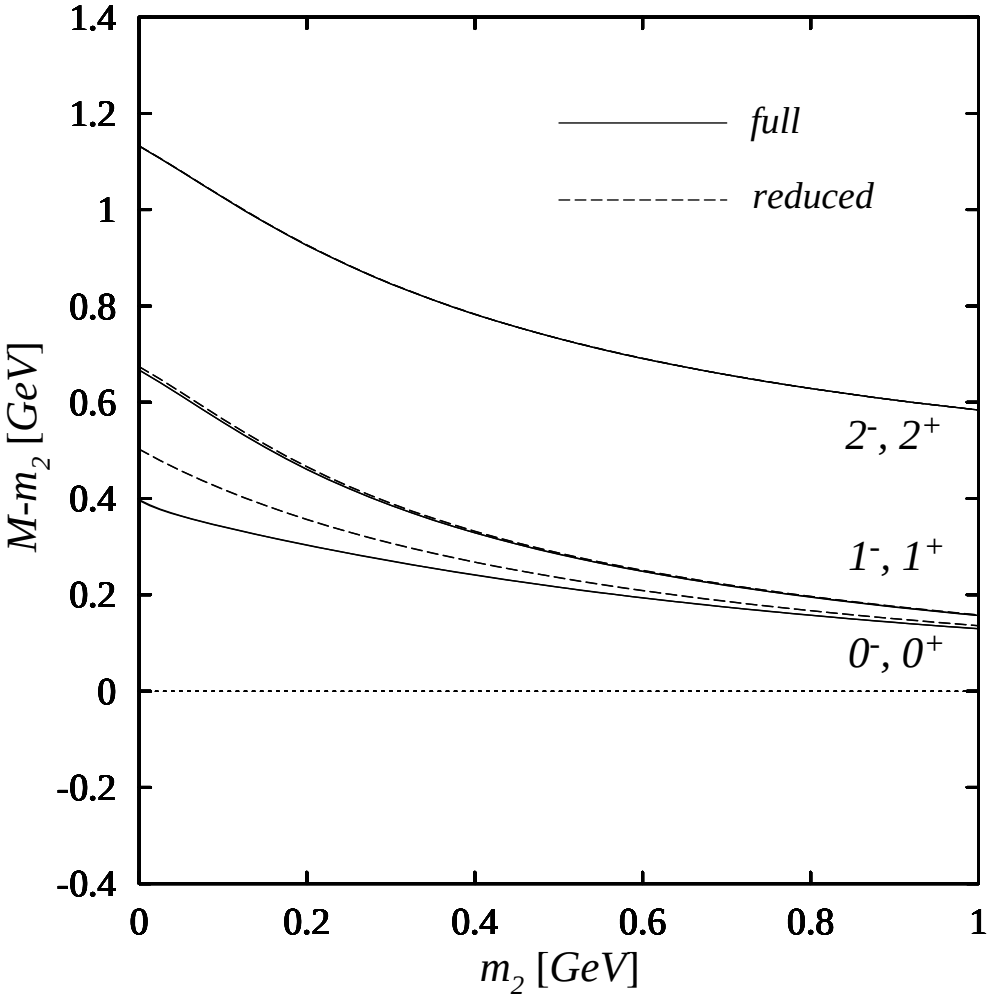
1.4
1.2
1
0.8
0.6
0.4
0.2
0
-0.2
-0.4
0
0.2
0.4
0.6
0.8
1
M-m2 [GeV]
m2 [GeV]
full
reduced
2-, 2+
1-, 1+
0-, 0+

Figure 6

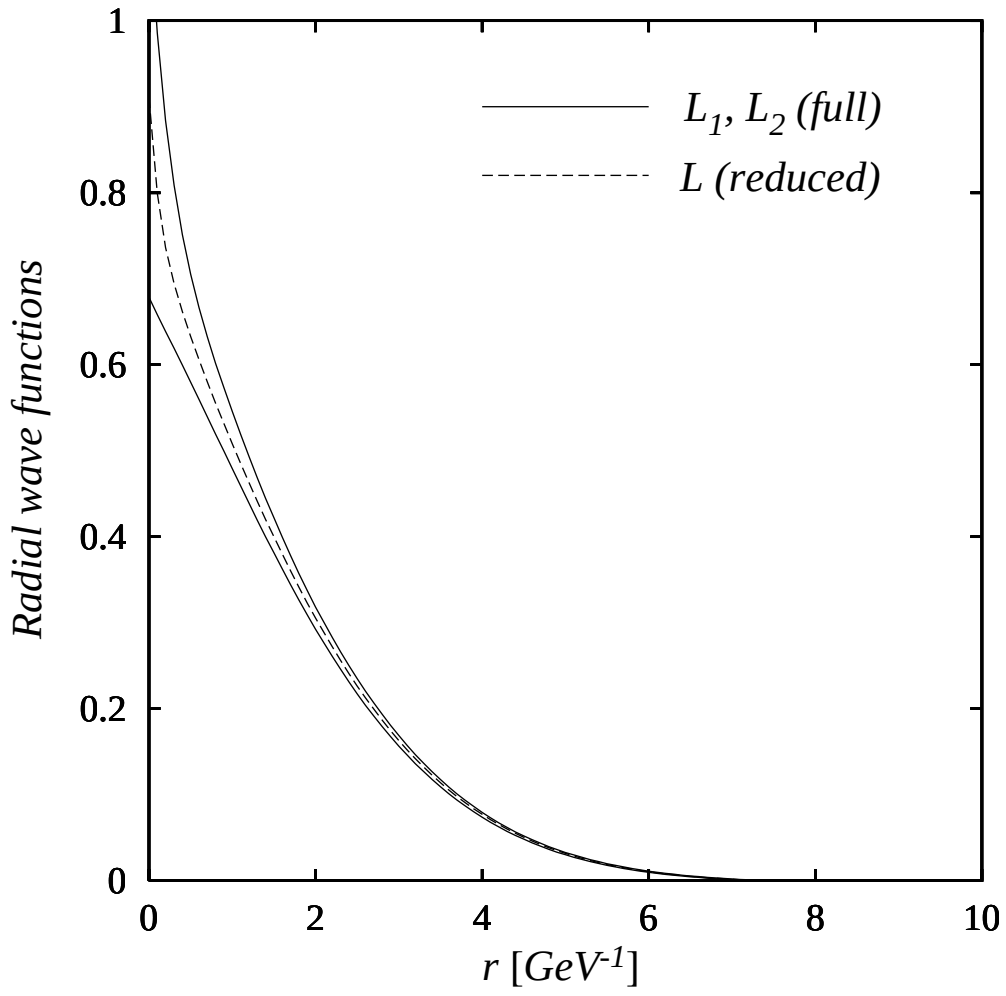
1
0.8
0.6
0.4
0.2
0
0
2
4
6
8
10
Radial wave functions
r [GeV-1]
L1, L2 (full)
L (reduced)

Figure 7

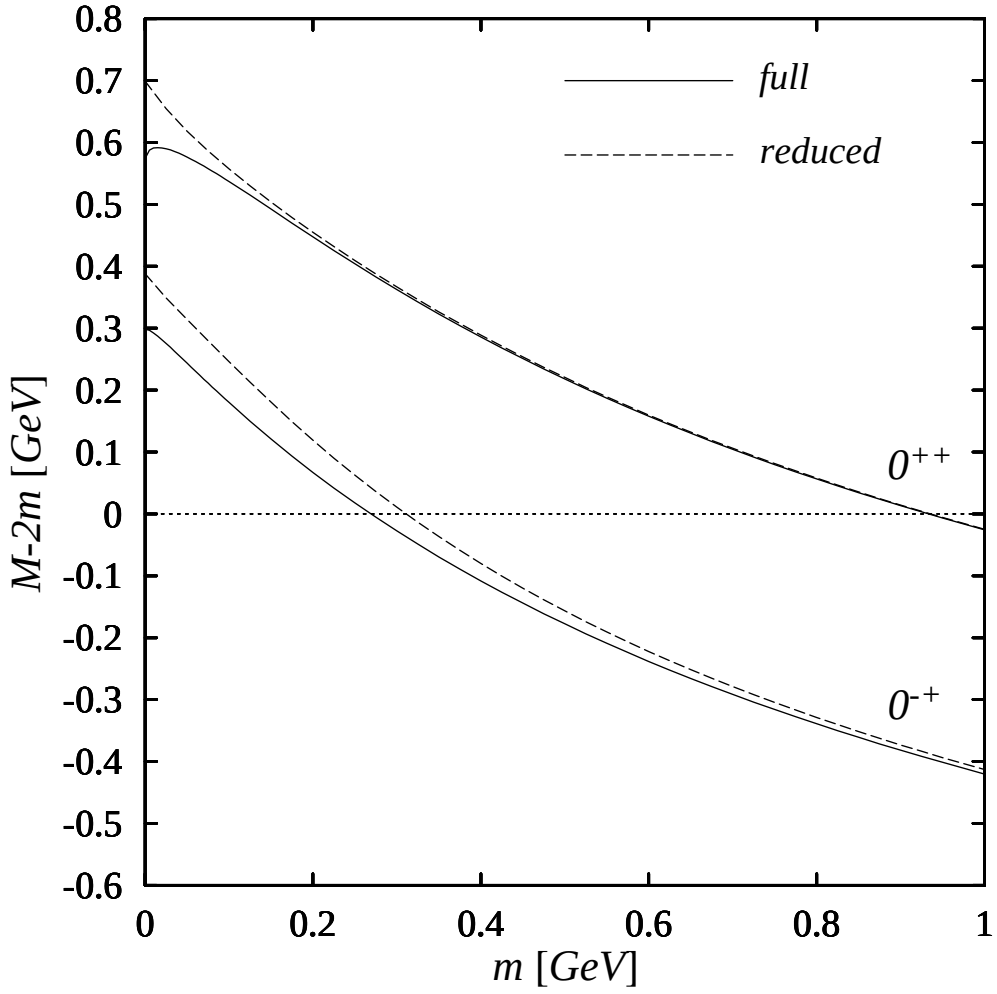
full
reduced
0^{++}
0^{-+}
M-2m [GeV]
m [GeV]
0.8
0.7
0.6
0.5
0.4
0.3
0.2
0.1
0
-0.1
-0.2
-0.3
-0.4
-0.5
-0.6
0
0.2
0.4
0.6
0.8
1

Figure 8

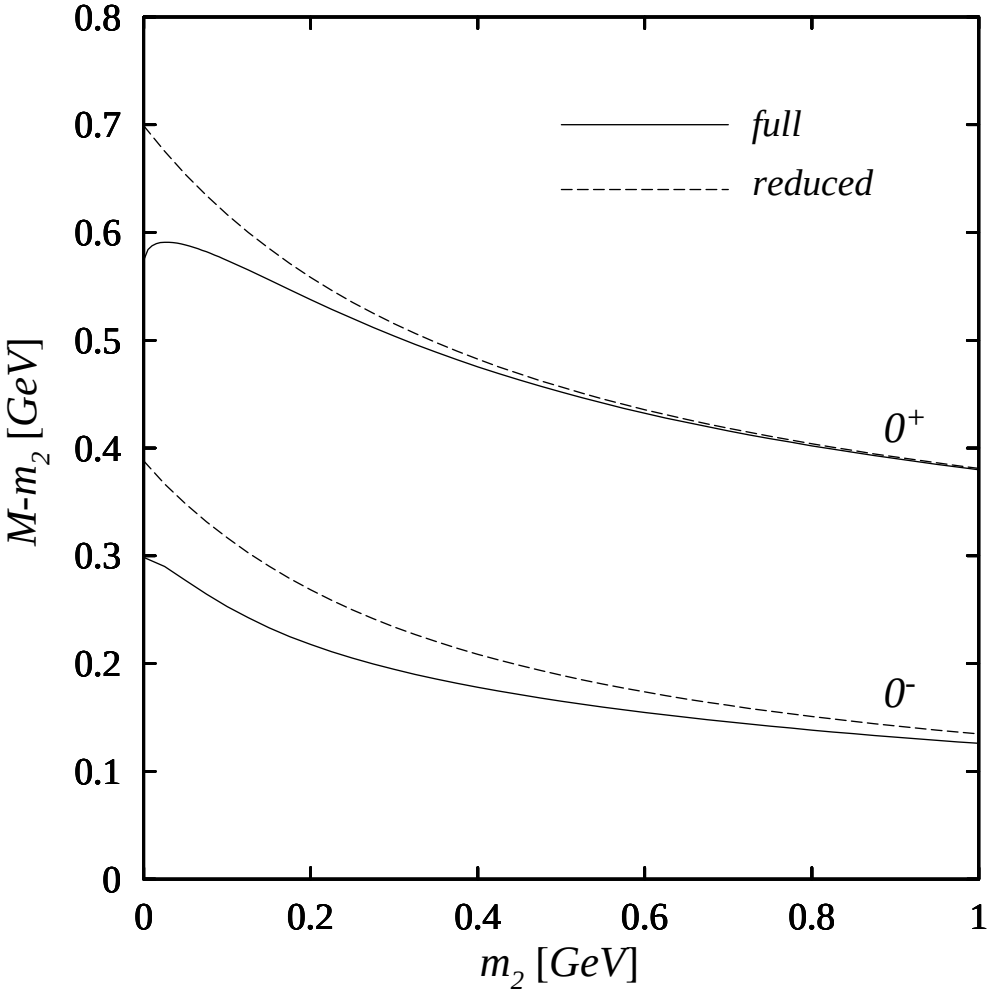
0.8
0.7
0.6
0.5
0.4
0.3
0.2
0.1
0
0
0.2
0.4
0.6
0.8
1
M-m2 [GeV]
m2 [GeV]
full
reduced
0+
0-

Figure 9

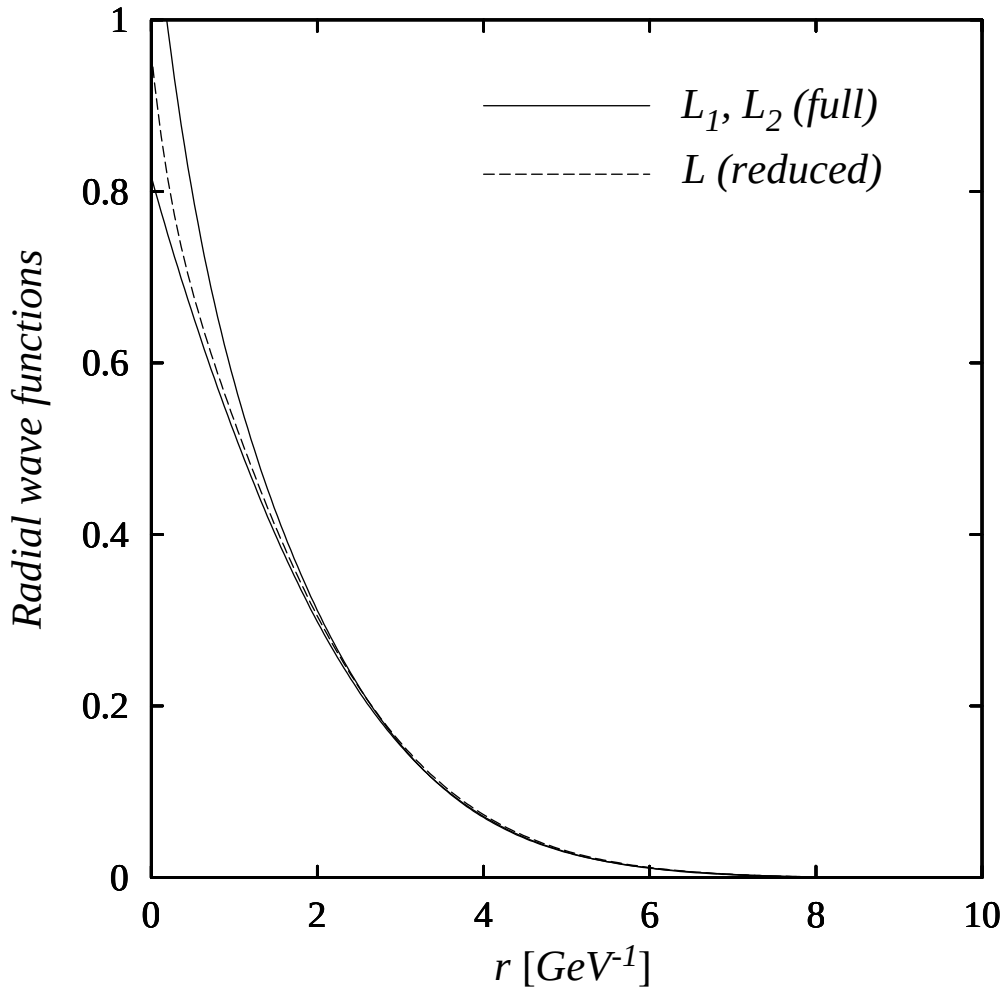
Radial wave functions
r [GeV-1]
L1, L2 (full)
L (reduced)
0
0.2
0.4
0.6
0.8
1
0
2
4
6
8
10

Figure 10

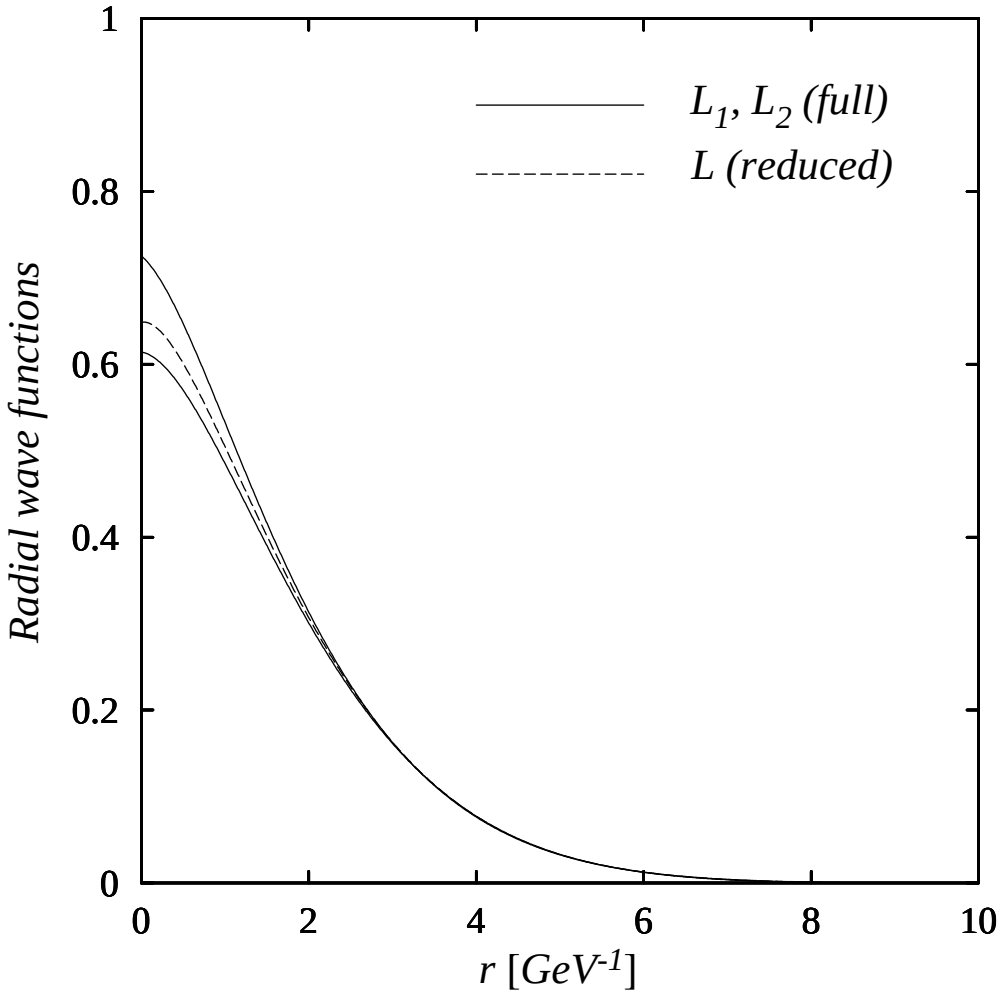
1
0.8
0.6
0.4
0.2
0
0
2
4
6
8
10
Radial wave functions
r [GeV-1]
L1, L2 (full)
L (reduced)

Figure 11

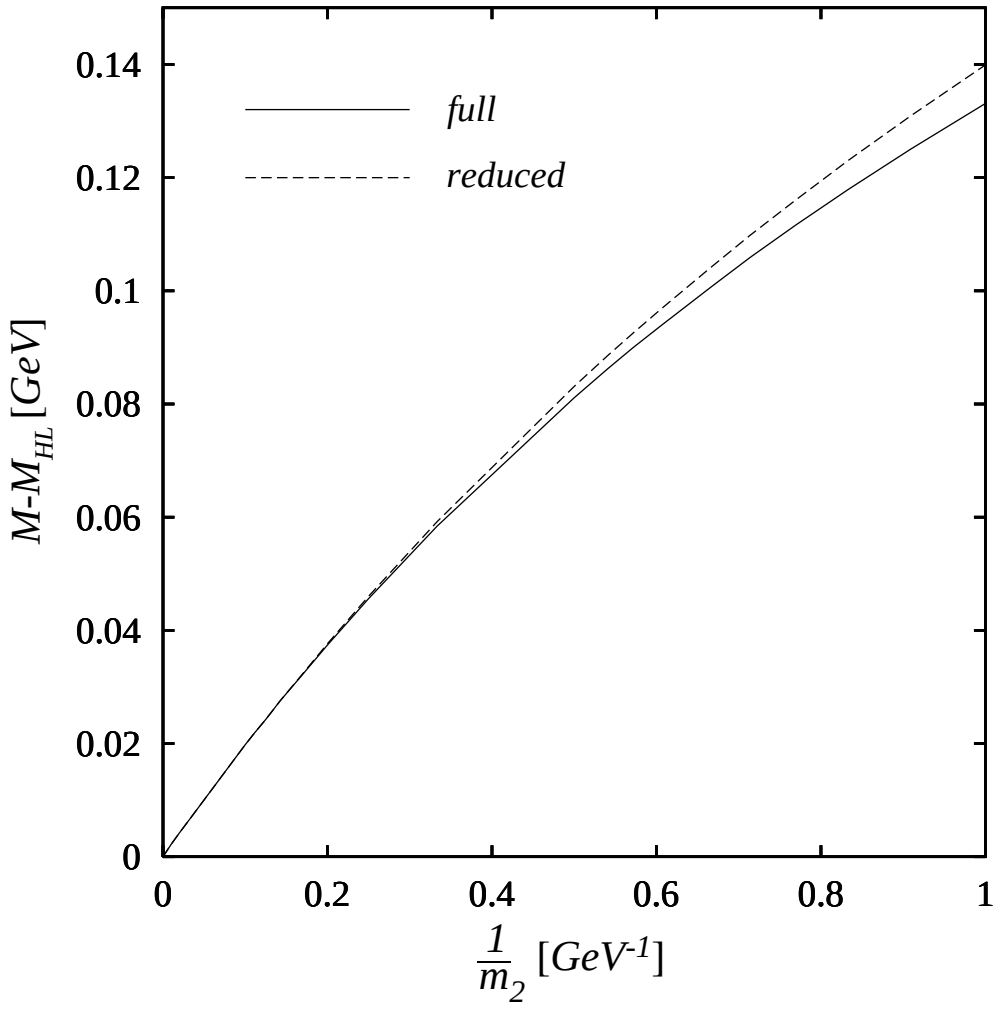
0.14
0.12
0.1
0.08
0.06
0.04
0.02
0
0
0.2
0.4
0.6
0.8
1
full
reduced
M-M_HL [GeV]
1/m_2 [GeV^-1]

Figure 12